Development 138, 4411-4422 (2011) doi:10.1242/dev.070979

Dynamic localization of *C. elegans* TPR-GoLoco proteins mediates mitotic spindle orientation by extrinsic signaling

Adam D. Werts, Minna Roh-Johnson and Bob Goldstein*

SUMMARY

Cell divisions are sometimes oriented by extrinsic signals, by mechanisms that are poorly understood. Proteins containing TPR and GoLoco-domains (*C. elegans* GPR-1/2, *Drosophila* Pins, vertebrate LGN and AGS3) are candidates for mediating mitotic spindle orientation by extrinsic signals, but the mechanisms by which TPR-GoLoco proteins may localize in response to extrinsic cues are not well defined. The *C. elegans* TPR-GoLoco protein pair GPR-1/2 is enriched at a site of contact between two cells – the endomesodermal precursor EMS and the germline precursor P_2 – and both cells align their divisions toward this shared cell-cell contact. To determine whether GPR-1/2 is enriched at this site within both cells, we generated mosaic embryos with GPR-1/2 bearing a different fluorescent tag in different cells. We were surprised to find that GPR-1/2 distribution is symmetric in EMS, where GPR-1/2 had been proposed to function as an asymmetric cue for spindle orientation. Instead, GPR-1/2 is asymmetrically distributed only in P_2. We demonstrate a role for normal GPR-1/2 localization in P_2 division orientation. We show that MES-1/Src signaling plays an instructive role in P_2 for asymmetric GPR-1/2 localization and normal spindle orientation. We ruled out a model in which signaling localizes GPR-1/2 by locally inhibiting LET-99, a GPR-1/2 antagonist. Instead, asymmetric GPR-1/2 distribution is established by destabilization at one cell contact, diffusion, and trapping at another cell contact. Once the mitotic spindle of P_2 is oriented normally, microtubule-dependent removal of GPR-1/2 prevented excess accumulation, in an apparent negative-feedback loop. These results highlight the role of dynamic TPR-GoLoco protein localization as a key mediator of mitotic spindle alignment in response to instructive, external cues.

KEY WORDS: Cell polarization, Cell-cell signaling, Mitotic spindle orientation

INTRODUCTION

Normal division orientation of metazoan cells is essential for cell diversification, development of normal tissue organization and tissue homeostasis (Siller and Doe, 2009). A growing body of evidence suggests that misregulating cell division orientation contributes to cancer development (Pease and Tirnauer, 2011). Cell divisions are commonly oriented by regulation of mitotic spindle orientation, regulation that in some cases depends on cell interactions (Goldstein, 1995; Schlesinger et al., 1999; Goldstein et al., 2006; Gomes et al., 2009; Inaba et al., 2010).

In diverse animal systems, a conserved protein complex has been implicated in orienting mitotic spindles and thus the mitotic division plane (Colombo et al., 2003; Gotta et al., 2003; Srinivasan et al., 2003; Lechler and Fuchs, 2005; Nguyen-Ngoc et al., 2007; Zhang et al., 2008; Hao et al., 2010; Oliaro et al., 2010; El-Hashash et al., 2011; Peyre et al., 2011; Williams et al., 2011). This complex is composed of a plasma membrane-anchored Gα protein (GPA-16 and GOA-1 in *C. elegans*) that binds a TPR-GoLoco protein (in *C. elegans*, two nearly identical proteins, GPR-1 and GPR-2; we use 'GPR-1/2' to refer to the protein pair), which links to microtubules through a microtubule associated protein (LIN-5 in *C. elegans*) and dynein, and/or through the Discs large protein and a kinesin (Siller and Doe, 2009). In most cases, the TPR-GoLoco protein is the most upstream component of the complex with asymmetric cortical localization. Thus, its localization is likely to be key in determining where this complex is active. This protein complex serves as a plasma membrane-anchored microtubule-binding complex, which is necessary for generating pulling forces on astral microtubules, resulting in orientation of mitotic divisions towards specific areas of the cell cortex (Grill et al., 2001; Pecreaux et al., 2006). In many cases, TPR-GoLoco proteins localize at specific cell-cell contacts towards which mitotic spindles align, suggesting that intercellular signaling at these contacts might localize TPR-GoLoco proteins. We would like to know whether extrinsic signaling provides instructive information, important for positioning for TPR-GoLoco protein localization and spindle orientation, or, alternatively, whether extrinsic signals function merely as permissive cues, not providing spatial information for TPR-GoLoco protein localization.

TPR-GoLoco proteins have been identified as key regulators of normal division in many systems (Fig. 1A). In vertebrate epithelial cell divisions in skin, lung, neuroepithelia and developing cysts, as well as in T cells, TPR-GoLoco proteins are positioned at specific locations (Lechler and Fuchs, 2005; Zhang et al., 2008; Hao et al., 2010; El-Hashash et al., 2011; Peyre et al., 2011; Williams et al., 2011), and are required for normal spindle orientation. In mammalian cysts, mislocalization of Gα results in the mislocalization of both the associated TPR-GoLoco protein, called LGN, and the mitotic spindle (Zheng et al., 2010), suggesting that the position of the TPR-GoLoco protein is important for cell division orientation. None of the systems listed above examines whether TPR-GoLoco protein localization is responding to extrinsic cues or, alternatively, whether cell contact positions merely coincide with the positions of internal polarity signals. Distinguishing between these possibilities will require experiments in which TPR-GoLoco protein localization is followed after cell contacts and/or intercellular signals are moved to new positions.

Biology Department, University of North Carolina at Chapel Hill, Chapel Hill, NC 27599, USA.

*Author for correspondence (bobg@unc.edu)

Accepted 1 August 2011

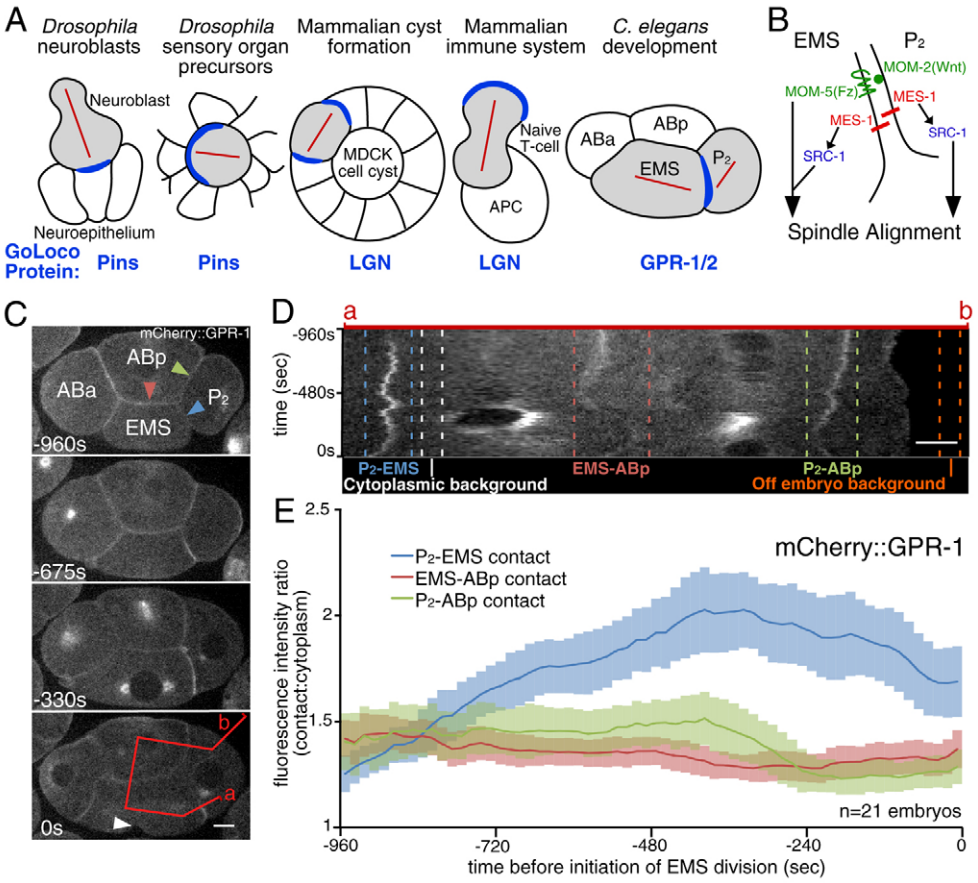

Fig. 1. Live imaging of tagged GPR-1 accurately reports the dynamic localization of endogenous GPR-1. (**A**) Schematic of TPR-GoLoco protein localization (blue) in several systems where these proteins function in spindle orientation (red). (**B**) Schematic of intercellular signaling between P_2 and EMS. (**C**) Live imaging of mCherry::GPR-1 from the birth of P_2 and EMS (–960s) to EMS division (0 seconds, arrowhead in bottom panel). Colored arrowheads mark specific cell contacts; red line indicates from where the kymograph in D was generated. (**D**) Kymograph from embryo in C. Fluorescence intensities between pairs of same-colored dotted lines were used to measure mCherry::GPR-1 signals at borders of interest. (**E**) Quantification of mCherry::GPR-1 signal from kymographs, generated from multiple embryos as in D. Error bars indicate 95% confidence intervals. Scale bars: 5 μm.

In only one case has it been clearly demonstrated that TPR-GoLoco proteins are positioned by instructive, extracellular cues during spindle orientation. In *Drosophila* sensory organ precursor cells (SOPs), extrinsic cues act through planar cell polarity (PCP) proteins Van Gogh, Frizzled and Flamingo to orient the mitotic spindle, and the localization of a TPR-GoLoco protein, Pins, has been implicated in division orientation (Chen et al., 2008; Gomes et al., 2009). Intercellular signals have been moved experimentally in this system by generating clones of cells that lack Van Gogh or Frizzled. Cells at the edges of these patches localize the TPR-GoLoco protein in ectopic positions that depend on the orientation of intercellular PCP signaling (Gomes et al., 2009), and the axis of mitotic division is altered. This result demonstrates a clear instructive effect of intercellular signaling on the positioning of a TPR-GoLoco protein. Is this representative of a general mechanism by which cell-cell signaling can orient mitotic spindles in animal systems? Do other systems use instructive signaling to position TPR-GoLoco proteins? What are the mechanisms of TPR-GoLoco protein localization in such systems? We are addressing these questions that are central to understanding how cell-cell signaling orients mitotic spindles, using the four-cell stage *C. elegans* embryo.

In the four-cell stage *C. elegans* embryo, two cells use intercellular signaling to orient their mitotic spindles towards a shared cell-cell contact (Goldstein, 1995; Arata et al., 2010) (Fig. 1A). A germline precursor cell, P_2, signals to an endomesodermal precursor, EMS, via two signaling pathways, a Wnt pathway and a MES-1 pathway (a novel receptor tyrosine kinase-like transmembrane protein that functions upstream of a Src kinase, SRC-1). EMS, in turn, signals to P_2 via MES-1 (Thorpe et al., 1997; Schlesinger et al., 1999; Berkowitz and Strome, 2000) (Fig. 1B). MES-1 is required for GPR-1/2 enrichment at the P_2-EMS contact (Srinivasan et al., 2003; Tsou et al., 2003), and this is assumed to reflect an asymmetric accumulation of GPR-1/2 within at least the EMS cell (Srinivasan et al., 2003; Tsou et al., 2003; Rose and Basham, 2006; Galli and van den Heuvel, 2008; Segalen and Bellaiche, 2009). MES-1 is required in both the P_2 and EMS cells for normal EMS division orientation, and it is also required for normal P_2 division orientation (Berkowitz and Strome, 2000; Srinivasan et al., 2003; Tsou et al., 2003; Arata et al., 2010) (Fig. 1B). GPR-1/2 has been implicated in normal EMS division as inactivating one of its cortical tethers, the Gα protein GPA-16, or inactivating a cortical antagonist, the DEP-domain protein LET-99, results in spindle orientation defects (Tsou et al., 2003); however, it is unknown whether P_2 division is also affected.

In this paper, we present the first high-resolution time-lapse imaging of a TPR-GoLoco protein involved in cell division orientation as it localizes in response to intercellular signaling. We demonstrate that GPR-1/2 does not localize asymmetrically in the endomesodermal precursor cell EMS, contrary to expectations (Srinivasan et al., 2003; Tsou et al., 2003; Rose and Basham, 2006; Galli and van den Heuvel, 2008; Segalen and Bellaiche, 2009). Instead, it localizes asymmetrically in P_2. We then sought to address three questions that are central to understanding how cell-cell signaling orients mitotic spindles, in a single system: does the TPR-GoLoco protein mediate spindle orientation by intercellular signaling? If so, is the TPR-GoLoco protein positioned instructively or permissively by extracellular signals? How is asymmetric localization of the TPR-GoLoco protein achieved? We demonstrate

that GPR-1/2 functions in centrosome positioning in the germline precursor, and that the normal distribution of GPR-1/2 in this cell is important for normal development. We show that intercellular signaling via MES-1/SRC-1 plays an instructive role in localizing GPR-1/2. Asymmetric GPR-1/2 localization is established by destabilization at one cortical site, diffusion and stabilization at another cortical site. Once the mitotic spindle is oriented normally, microtubule-dependent removal of GPR-1/2 prevents its excessive accumulation. Our results demonstrate that dynamic localization of GPR-1/2 can serve as an intermediate that relays positional information from intercellular signaling to the alignment of a mitotic spindle, and it sheds light on mechanisms of asymmetric TPR-GoLoco protein localization downstream of extrinsic signals.

MATERIALS AND METHODS

Strains

Strains (see Table S1 in the supplementary material) were maintained at 20°C as described previously (Brenner, 1974). Sterility tests were carried out at 25°C. Temperature-sensitive alleles were shifted to 25°C during the two-to-three cell stage for *gpa-16(it143)* or just after birth of P_2 and EMS for *spd-2(or188)*.

Imaging

Images were acquired as described previously (McCarthy Campbell et al., 2009), except embryos were illuminated with 488 nm, 514 nm or 568 nm light using a water-cooled Innova 70C Spectrum laser, and images were acquired every 15 seconds. Images were acquired using a 60× Plan Apo 1.4NA objective (Nikon), except worm images in Fig. 4D, which were acquired using DIC optics on a Nikon Eclipse E800 with a 20× Plan Fluor 0.50NA objective (Nikon) and a Spot Insight 2-Megapixel camera. FRAP was carried out on an inverted Eclipse TE2000 (Nikon) with a multi-beam confocal imaging system (VT-HAWK; VisiTech) using a 25 mW solid-state 491 nm laser and a 16-bit cooled CCD camera (Orca R2; Hamamatsu). A 3.5×3.5 μm region of interest (ROI) was photobleached at 100% laser power for 400-650 ms. Images were acquired at 1-second intervals starting 183 mseconds after photobleaching. In Fig. 7 and Fig. S6 in the supplementary material, 'early' FRAP is 720-540 seconds prior to initiation of EMS division, and 'late' FRAP is 270-290 seconds before initiation of EMS division.

Analysis and quantification of imaging

Intact embryos

Using Metamorph, the average values along a three pixel wide linescan passing perpendicularly through each border of interest (the brightest region of the P_2-EMS contact, and the center of the P_2-ABp and EMS-ABp contacts), through the cytoplasm and through off-embryo background were used to generate a kymograph of the time-lapse (Fig. 1C,D). From the kymograph, maximal pixel intensities along each cell-cell contact, as well as average cytoplasmic and background signal intensities were recorded. Cytoplasmic signal and cell-cell contact signals were calculated by subtracting off-embryo pixel intensities. The start of EMS division was defined here as when the indentation of cytokinesis was first seen.

Cell manipulations

Quantification of GPR-1 signal at P_2-EMS contacts, as in Figs 2 and 3, was carried out using the method of Hoffman et al. (Hoffman et al., 2001). Three independent measurements just prior to P_2 alignment were taken and averaged as the measurement for that recombination. As this method does not work well for signal at curved membranes, quantification of GPR-1 signal in Fig. S4 in the supplementary material was carried out as follows: a 5 pixel wide ROI was drawn to encompass each region depicted in Fig. S4 in the supplementary material, or a region of the cytoplasmic signal. Maximal pixel intensities were recorded along that line for three separate time points during a 90-second time window around maximal accumulation of GPR-1 at the endogenous P_2-EMS contact. The average of these pixels values was reported as the value for that membrane in that experiment. All graphs and data analysis were made in Excel.

FRAP

Fluorescence intensity in photobleached areas was calculated as a ratio over cytoplasmic background and normalized to 100% at t=–1 second for each FRAP experiment. Normalized FRAP curves for each experiment were adjusted for non-specific photobleaching owing to imaging conditions, as demonstrated in Fig. S5A-C in the supplementary material, plotted with Prism 5 (GraphPad Software), and fitted with one-phase exponentials. Embryos that showed an overexpression phenotype as in Fig. 4 were excluded from FRAP analysis.

Immunofluorescence and western blotting

Immunostaining was carried out as described by Tenlen et al. (Tenlen et al., 2008) but with a 15-minute fix in 50% acetone and 50% methanol at –20°C, and the secondary fix time was reduced to 4 minutes. Antibodies and dilutions used were: DM1α 1:300 (Sigma-Aldrich), GPR-2 1:300 [a gift from Monica Gotta (Gotta et al., 2003)], Rhodamine Red-X goat anti-mouse 1:2000 (Invitrogen), Cy2-conjugated goat anti-rabbit 1:2000 (Millipore). For western blotting, antibodies and dilutions used were as follows: DM1α 1:1500, GPR-2 from Gotta et al. (Gotta et al., 2003) 1:1000, αEGFP 1:500 (Clontech, #632569), αmCherry 1:100 (Clontech, #632543), ECL peroxidase-labeled anti-rabbit 1:2000 (GE Healthcare) and ECL peroxidase-labeled anti-mouse 1:2000 (GE Healthcare). For both immunofluorescence and western blotting, GPR-2 antibodies, received as gifts from the van den Heuvel Lab (Srinivasan et al., 2003) and the Rose Lab (Tsou et al., 2003), were also tested with similar results (data not shown).

Cell manipulations

Cell isolations were preformed as described by Edgar (Edgar, 1995), with the following alteration: chitinase from *Serratia marcescens* was substituted with chitinase from *Streptomyces griseus* (Sigma, C6137) at a concentration of 10 U/ml. Pairs of P_2-EMS sister cells were recombined between 2 and 4 minutes after completion of division, as judged visually under a dissecting microscope. Cells were mounted in Shelton's growth media (Shelton and Bowerman, 1996) and imaged as described above.

Defining alignment of P_2 and EMS as in Fig. 3

EMS

Both centrosomes in a single EMS cell were scored as aligned toward both P_2 cells if both ends of the mitotic spindle, or the two resulting nuclei forming in telophase of EMS division, were closer to the P_2 cells than was a line drawn from the outer edge of one P_2-EMS contact through the EMS cell to the other P_2-EMS contact. EMS cells were scored as aligned towards only the sister cell or only the ectopic contact if they had one centrosome beyond this line when EMS started division or one nucleus beyond this line at telophase.

P_2

One end of the P_2 spindle was considered aligned toward both EMS cells when one of the centrosomes rocked back and forth between one EMS and the other prior to initiating division. Alignment towards only one EMS cell was scored when one P_2 centrosome moved towards one EMS cell without showing motion towards the other EMS cell. Alignments were reported only for cell manipulations where the two sets of P_2-EMS pairs divided within 3 minutes of one another, as we found that larger differences in age between P_2-EMS pairs showed different patterns of divisions in P_2 and EMS: older sister pairs tended to align toward one-another, whereas very young sister pairs tended to align toward older pairs (data not shown).

RNAi

dsRNA preparation and injection was carried out as described previously (Dudley et al., 2002). dsRNA feeding was carried out as described previously (Sawyer et al., 2011).

Nocodazole

Embryos were preameabilized for drug delivery as described by Hill and Strome (Hill and Strome, 1988), except embryonic culture medium was replaced with Shelton's medium (Shelton and Bowerman, 1996). Nocodazole (Sigma) (2 mM stock) in DMSO was dissolved in Shelton's medium to a final concentration of 40 μM. This concentration was found

to depolymerize astral microtubules sufficiently in a YFP::α-tubulin strain (data not shown). Nocodazole was applied as described by McCarthy Campbell et al. (McCarthy Campbell et al., 2009). Embryos were imaged from the birth of P_2 and EMS until several minutes after when EMS would have normally divided.

Statistics

All bar and line graphs are presented with error bars representing 95% confidence intervals. All reported *P*-values were calculated by using two-tailed Student's *t*-tests in Excel.

RESULTS

Live imaging of transgenic GPR-1 accurately reports the dynamic enrichment of GPR-1/2 at the P_2-EMS contact

GPR-1/2 has been imaged previously in fixed four-cell stage embryos (Srinivasan et al., 2003; Tsou et al., 2003). To understand how a TPR-GoLoco protein becomes localized dynamically in response to intercellular signaling, we imaged living embryos expressing mCherry::GPR-1 or YFP::GPR-1 (Fig. 1; see Movie 1 and Fig. S1D in the supplementary material), both of which were designed with *C. elegans* codon bias (Redemann et al., 2010). GPR-1 and GPR-2 are nearly identical proteins (Colombo et al., 2003); we use GPR-1/2 to refer to the endogenous protein pair and GPR-1 to refer to our transgenic versions. mCherry::GPR-1 and YFP::GPR-1 appear to be reliable proxies for endogenous protein localization and function. First, both transgenes produced proteins of the expected size (see Fig. S1C in the supplementary material). Second, the tagged proteins localize in the same pattern as endogenous protein at the four-cell stage (compare Fig. 1C-E with Fig. S1D and Fig. S3 in the supplementary material), and we found that they can rescue knockdown of endogenous *gpr-1/2* by RNAi (see Fig. S1 in the supplementary material). Third, like endogenous GPR-1 (Srinivasan et al., 2003; Tsou et al., 2003), mCherry::GPR-1 enrichment is dependent on MES-1/SRC-1 signaling and not on Wnt signaling (see Fig. S2A-F in the supplementary material).

GPR-1 is localized asymmetrically in the P_2 cell, not the EMS cell, and is positioned instructively by MES-1 signaling

Results showing that MES-1/SRC-1 signaling is required for normal alignment of both P_2 and EMS divisions (Srinivasan et al., 2003; Tsou et al., 2003; Arata et al., 2010) suggested that GPR-1/2 might be asymmetrically enriched at the P_2-EMS contact in both the P_2 and EMS cells. To identify the cell(s) of origin of the GPR-1 signal and to determine the role of signaling in positioning GPR-1, we created mosaics composed of different GPR-1 fluorescent reporters by combining dissected P_2-EMS pairs in specific orientations (Fig. 2). First, we tested whether we could experimentally recruit GPR-1 to ectopic sites with ectopic cell contacts. We combined two pairs of P_2-EMS cells expressing mCherry::GPR-1 in an antiparallel orientation (Fig. 2A) and found that ectopic P_2-EMS contacts (contacts between non-sister P_2-EMS cells) and endogenous P_2-EMS contacts (contacts between sister P_2-EMS cells) recruited indistinguishable levels of protein (Fig. 2B). This result suggests that the ectopic P_2-EMS contacts can recruit GPR-1 as endogenous P_2-EMS contacts do, and hence that cell-cell contact can enrich GPR-1 at a cortical site. This appears to depend on MES-1 signaling specifically at the P_2-EMS contact, as control recombinations between P_2-EMS pairs and the other two cells of the four-cell stage – ABa and ABp – referred to as ABx here, and contacts with P_2-EMS pairs that lack MES-1 failed to accumulate similar levels of mCherry::GPR-1 (Fig. 3A,E,F). We conclude that MES-1 signaling at ectopic P_2-EMS contacts can recruit cortical GPR-1 to levels comparable with levels at endogenous P_2-EMS contacts.

To test whether the ectopic accumulation of GPR-1 arises due to accumulation in the EMS cell, the P_2 cell, or both, we combined P_2-EMS half-embryo sister-pairs in which each pair contained a distinct fluorescent label on GPR-1 (Fig. 2C,C′; see Movie 2 in the supplementary material). Observation of these mosaics suggested that the P_2 cell contributed most of the GPR-1 signal to the P_2-EMS contact (Fig. 2C′). To assess this quantitatively, we combined labeled P_2-EMS sister pairs with unlabeled wild-type P_2-EMS sister pairs as described above. We found that P_2 contributed significantly more GPR-1 signal than EMS, using either the mCherry::GPR-1 or YFP::GPR-1 strains (Fig. 2D-G). Surprisingly, GPR-1 is not asymmetrically distributed in the EMS cell (Fig. 2D′,F′; see Fig. S4 in the supplementary material). We conclude that the TPR-GoLoco protein, GPR-1/2, is asymmetrically localized in the P_2 cell, and not in the EMS cell.

The normal distribution of GPR-1 in P_2 is important for spindle alignment and germline development

We sought to test whether TPR-GoLoco protein asymmetry is required for normal asymmetric division of the P_2 cell. We showed above that specific cell contacts and MES-1 are required for GPR-1 localization in the P_2 cell. In these experiments, we noticed that spindle orientation in P_2 similarly depended on specific cell contacts and MES-1 (Fig. 3A-D), consistent with previous work on P_2 division asymmetry (Arata et al., 2010). The parallel effects on GPR-1 localization and spindle alignment might reflect a requirement for GPR-1/2 in spindle alignment. To test this hypothesis, we interfered with GPR-1/2 localization. Because GPR-1/2 is required earlier at the one-cell stage (Grill et al., 2003), we interfered with GPR-1/2 localization at the four-cell stage using *gpa-16(it143)*, a temperature-sensitive allele of one of the cortical Gα tethers of GPR-1/2. We found diminished GPR-1 accumulation at the P_2-EMS contact in upshifted *gpa-16(it143)* embryos (see Fig. S2D-F in the supplementary material), associated with spindle orientation defects in P_2 (Fig. 4A), consistent with a role for normally localized GPR-1 in the P_2 cell. As expected, a *mes-1* mutation produced a similar phenotype of diminished GPR-1 accumulation at the P_2-EMS contact (see Fig. S2B-F in the supplementary material) (Srinivasan et al., 2003; Tsou et al., 2003) and P_2 orientation defects (Fig. 4A). These experiments suggest that loss of GPR-1 asymmetry in P_2 results in P_2 division orientation defects.

We hypothesized that GPR-1/2 might regulate forces on microtubules at the four-cell stage, based on its role as a force-regulating component for spindle orientation at the one-cell stage (Grill et al., 2003). To test this, we determined whether excess GPR-1 at the P_2-EMS contact would result in specific defects in centrosome positioning by exploiting a YFP::GPR-1 strain that we found recruits excess GPR-1 to the P_2-EMS contact (Fig. 4B). In some YFP::GPR-1 embryos (6/48, 12.5%), we found that in the last four minutes before initiation of EMS division, the P_2 centrosome closer to the P_2-EMS contact dissociated from the nuclear envelope, moved toward the contact with EMS and then back to the nucleus; this repeated several times (Fig. 4C,D; see Movie 3 in the supplementary material). The other centrosome in P_2 and both centrosomes in EMS did not show this extreme oscillation. We never observed this oscillating behavior in wild-

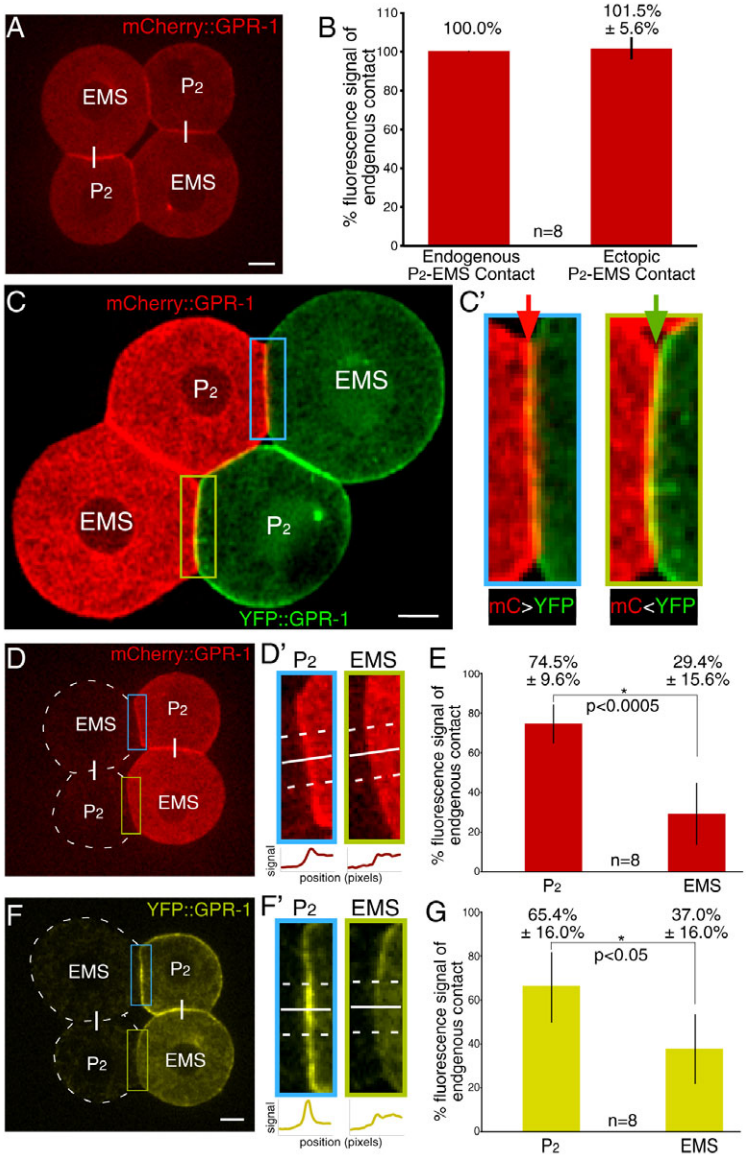

Fig. 2. GPR-1 is enriched in P_2 at the contact with EMS, positioned by cell contact. (**A**) Live imaging of mCherry::GPR-1 after manipulation of two P_2-EMS cell pairs into anti-parallel configuration. White lines mark sister-cell pairs. (**B**) Quantification of mCherry::GPR-1 signals at P_2-EMS contacts after cell manipulations as in A. Signals were normalized to that at the endogenous P_2-EMS contact. (**C**,**C′**) Similar cell manipulations with P_2-EMS pairs from mCherry::GPR-1 and YFP::GPR-1 strains. Colored arrows in C′ highlight the fluorescence signal in the cell that contributes more GPR-1 to that cell-cell contact. (**D**,**D′**) Live imaging of cell manipulations from two genetic backgrounds: wild type and mCherry::GPR-1. White lines connect sister-cell pairs and dotted white lines outline wild-type unlabeled cells. Colored-coded rectangles are expanded in D′ and quantified below from linescans (white lines) across contacts. (**E**) Quantification from manipulations as in D. (**F-G**) As in D-E, but with YFP::GPR-1-labeled cells. Scale bars: 5 μm. Error bars indicate 95% confidence intervals. Asterisks indicate statistical significance.

type embryos, in mCherry::GPR-1 embryos – which have a lower GPR-1 asymmetry at the time of centrosome alignment (Fig. 4B) – or in YFP::GPR-1; *src-1(RNAi)* embryos (0/22), suggesting that the oscillation is due to MES-1/SRC-1 signaling-dependent recruitment of excess GPR-1 in P_2 at the contact with EMS. The periodic nature of this movement appears similar to that of spindle oscillations seen when the mammalian homolog of GPR-1/2, LGN, is overexpressed in cell culture (Du and Macara, 2004), and similar to that of posterior centrosome oscillations caused by GPR-1/2-mediated pulling forces during the one-cell stage in *C. elegans* (Pecreaux et al., 2006) (Fig. 4D). This suggests that these abnormal centrosome movements might result from a similar increase in pulling forces at the site of contact with EMS in the presence of the additional GPR-1.

Increased GPR-1 at the P_2-EMS contact was also associated with developmental consequences. In *mes-1* animals, lack of GPR-1 enrichment at the P_2-EMS contact is associated with P_2 spindle orientation defects (Fig. 4A), missegregation of cytoplasmic germ granules and loss of germline development (Strome et al., 1995; Berkowitz and Strome, 2000; Srinivasan et al., 2003; Tsou et al., 2003). We found that some YFP::GPR-1 worms also developed without a functional germline (Fig. 4E), suggesting that too much or too little GPR-1/2 at the P_2-EMS contact may each result in the same terminal phenotype.

From these experiments we conclude: (1) GPR-1 binding sites at the P_2 side of the P_2-EMS contact are not normally saturated; (2) overexpressing GPR-1 can allow MES-1/SRC-1 signaling to recruit excess GPR-1 in P_2 to the contact with EMS; and (3) mislocalization of GPR-1 or excess GPR-1 are associated with spindle defects in P_2 and worms that develop without a functional germline. We conclude that the level of GPR-1/2 in P_2 at the site of contact with EMS is likely to be important in normal spindle orientation. These results prompted us to investigate how GPR-1/2 normally becomes localized asymmetrically.

MES-1/SRC-1 signaling and a cortical GPR-1 antagonist, LET-99, affect GPR-1 localization independently

To understand mechanisms of TPR-GoLoco protein localization, we began by examining a role for a known antagonist, the DEP domain protein LET-99 (Park and Rose, 2008). In the four-cell stage embryo, LET-99 becomes enriched at all cell-cell contacts

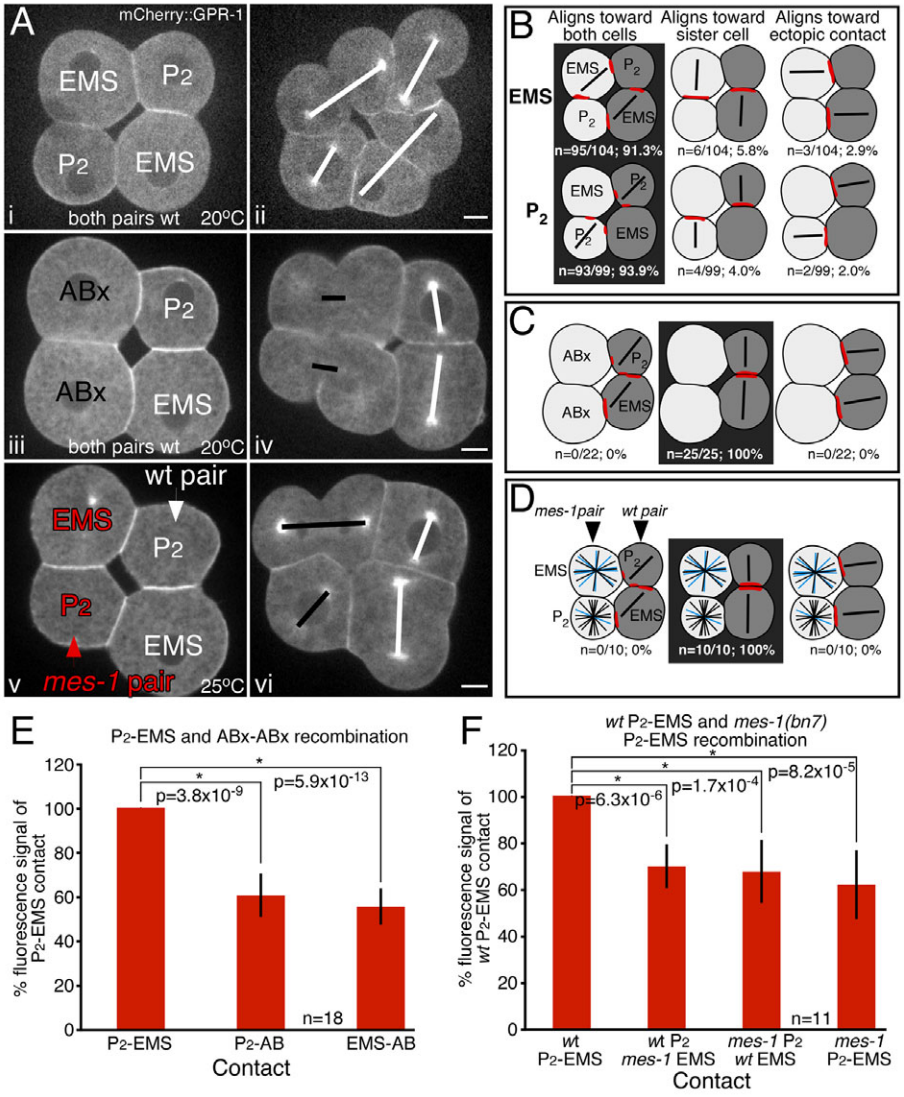

Fig. 3. MES-1 regulates GPR-1 accumulation and spindle orientation in P_2. (**A**) Still from live imaging of mCherry::GPR-1 cell manipulations: i and ii, two P_2-EMS pairs combined; iii and iv, one P_2-EMS pair combined with a control ABx pair; v and vi, one wild-type and one *mes-1(bn7)* P_2-EMS pair combined. Left column: before mitosis. Right column: as some cells divide. White line indicates centrosome alignment. Scale bars: 5 μm. (**B-D**) Division alignments (black lines) from experiments shown in A. Sister cell pairs are the same color. Red: cell-cell contacts towards which centrosomes moved. Black boxes highlight the most frequent alignment in each experiment. Blue lines in D indicate that some divisions initiated towards/away from the cover glass. (**E**) Quantification of mCherry::GPR-1 signal at cell-cell contacts from experiments as in Aiii. (**F**) Quantification of mCherry::GPR-1 signal at cell-cell contacts from experiments as in Av. Error bars indicate 95% confidence intervals. Asterisks indicate statistical significance.

except the P_2-EMS contact site, where GPR-1/2 is enriched (Tsou et al., 2003). In the one-cell embryo, LET-99 antagonizes GPR-1/2, preventing its cortical localization and downregulating GPR-1/2-mediated pulling forces on astral microtubules (Park and Rose, 2008).

We sought to test the hypothesis that MES-1/SRC-1 signaling acts through exclusion of LET-99 at the P_2-EMS contact, allowing GPR-1/2 enrichment (Tsou et al., 2003). Quantification of YFP::LET-99 revealed that transgenic YFP::LET-99 behaves like endogenous LET-99 (Tsou et al., 2003), with the level at the P_2-EMS contact being significantly lower than that at the other cell contacts (Fig. 5A,B; see Fig. S5A,F in the supplementary material). Upon reduction of MES-1/SRC-1 signaling by *mes-1(RNAi)* or *src-1(RNAi)*, the P_2-EMS contact no longer appeared to have more GPR-1/2 than other contacts, by examining both endogenous protein level (Srinivasan et al., 2003; Tsou et al., 2003) and mCherry::GPR-1 (Fig. 5D; see Fig. S5B,C,G in the supplementary material). However, we found that this change in GPR-1 level was not associated with an increased accumulation of YFP::LET-99 (Fig. 5C,D; see Movie 4 in the supplementary material). Because quantification of the YFP::LET-99 signal at the P_2-EMS contact revealed no significant difference between wild-type, *mes-1(RNAi)* or *src-1(RNAi)* backgrounds (Fig. 5C), we propose that MES-1/SRC-1 signaling does not affect the LET-99 level at the P_2-EMS contact. Moreover, reduced YFP::LET-99 at other contacts (EMS-ABp and P_2-ABp contacts) in *mes-1(RNAi)* and *src-1(RNAi)* embryos was not associated with local increases in mCherry::GPR-1 levels (see Fig. S5G in the supplementary material). From these experiments, we conclude that the effects of LET-99 (Tsou et al., 2003) and MES-1/SRC-1 signaling on GPR-1/2 localization at the four-cell stage are likely to be independent (Fig. 5E).

GPR-1 localizes asymmetrically by destabilization at one cell contact, diffusion and stabilization at another cell contact

How do TPR-GoLoco proteins become enriched at a specific cell-cell contact? Imaging mCherry::GPR-1 and YFP::GPR-1 at a central plane in the embryo (Fig. 1C,D; see Fig. S1D in the supplementary material), or at the cortical surface (Fig. 6D,D′) did not reveal any net movement of GPR-1 punctae or any cytoplasmic (Fig. 1D) or cortical flow of GPR-1 towards the P_2-EMS contact during the period of GPR-1 accumulation at this contact. Because labeled GPR-1 cannot be seen moving toward the P_2-EMS contact where it is accumulating, we sought a method to quantitatively measure changes in GPR-1 dynamics at this and other cell contacts

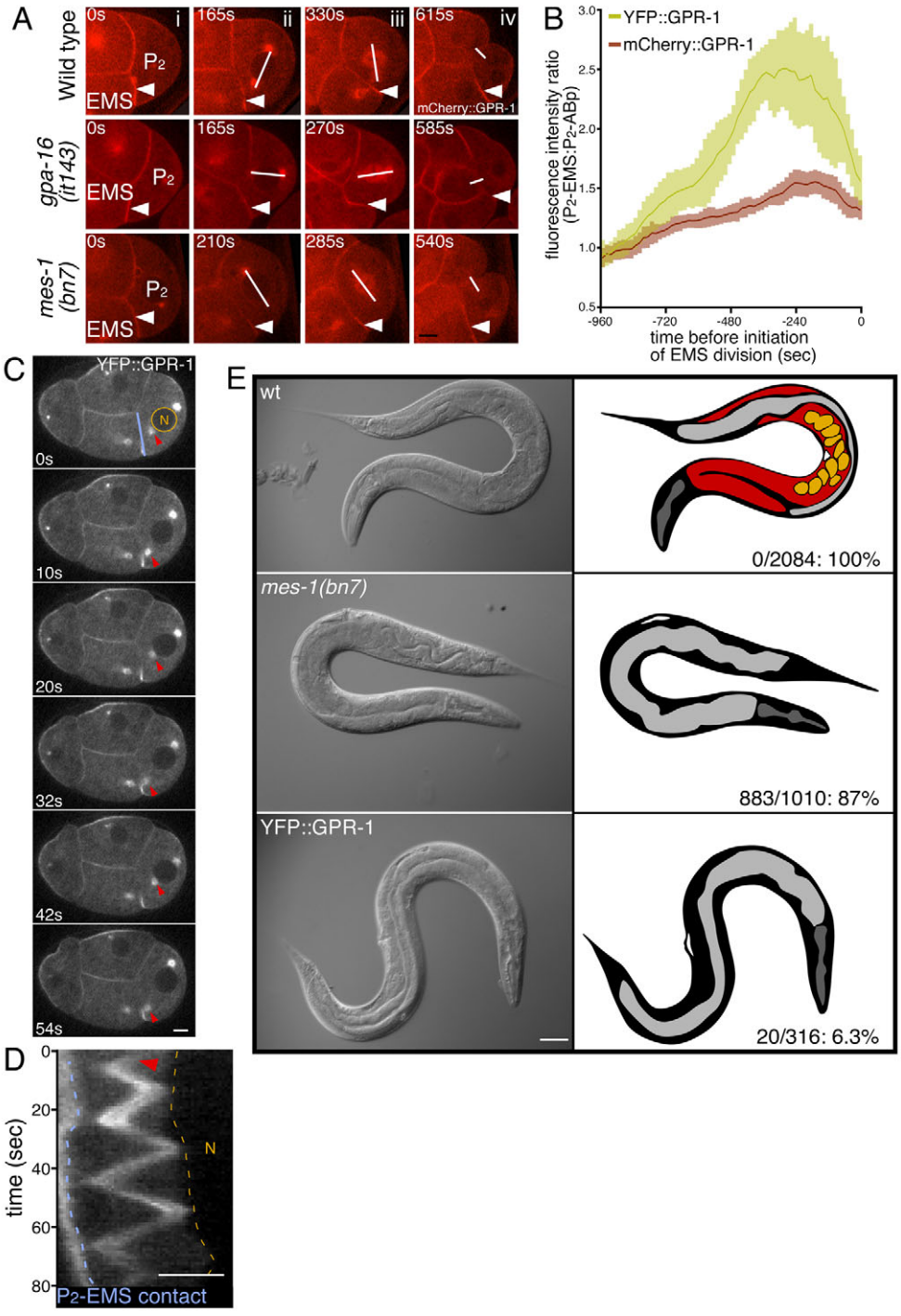

Fig. 4. Normal GPR-1 distribution in P_2 plays important roles in development. (**A**) Live imaging of embryos expressing mCherry::GPR-1 in different backgrounds. Upshifted *gpa-16(it143)* and *mes-1(bn7)* P_2 cells did not orient centrosomes towards the contact with EMS (white arrowheads). White lines connect diametrically opposed P_2 centrosomes (ii), spindle orientation at metaphase (iii) or sister cells resulting from P_2 division (iv). All images in A were taken at 25°C. (**B**) YFP::GPR-1 asymmetry is greater than mCherry::GPR-1 asymmetry, based on ratio of tagged GPR-1 at the P_2-EMS contact to that at the P_2-ABp contact in each strain. The ratio of signal at the P_2-EMS contact to that in the cytoplasm was also greater in our YFP::GPR-1 strain than in our mCherry::GPR-1 strain (Fig. 1E; see Fig. S1D in the supplementary material). Error bars indicate 95% confidence intervals. (**C**) Live imaging of YFP::GPR-1 showing centrosome defects seen in P_2. In some embryos, the P_2 centrosome nearer the contact with EMS (red arrowhead) detached from the nuclear envelope (yellow circle) and oscillated between the P_2-EMS contact (blue line) and the nucleus. Time is marked in seconds after oscillations began. (**D**) Kymograph of centrosome oscillations from C: centrosome (arrowhead); nuclear envelope (yellow dotted line); P_2-EMS contact (blue dotted line). The centrosome reached an average maximum velocity of 0.48±0.04 μm seconds^{-1}, n=6. (**E**) DIC images of adult worms raised at 25°C. Some YFP::GPR-1 worms phenocopy *mes-1(bn7)* worms, with no apparent germline as adults: gonad/germline (red); embryos (yellow); intestine (light gray); pharynx (dark gray). Scale bars: 100 μm in E; 5 μm in A-D.

over time. We performed FRAP experiments on YFP::GPR-1 at all cell-cell contacts of interest early and late during the P_2 and EMS cell cycles (Fig. 6A,B; see Materials and methods).

Our analysis revealed that all cell-cell contacts show recovery of GPR-1 to nearly 100% within 80 seconds, and little to no immobile fraction (see Fig. S6A-F in the supplementary material). Especially striking results were found when examining temporal changes in the rate of GPR-1 turnover at the P_2-EMS and P_2-ABp contacts, which showed complementary changes over time (Fig. 6C). The half-life of recovery ($t_{1/2}$) at the P_2-EMS contact lengthened more than three times from early in the cell cycle to late, as the $t_{1/2}$ at the P_2-ABp contact showed an inverse pattern, decreasing by half from early in the cell cycle to late (Fig. 6C; see Fig. S6F in the supplementary material). These results show that over time, YFP::GPR-1 associates more stably with the P_2-EMS contact and less stably with the P_2-ABp contact.

Together, lack of punctae movement or flow of protein toward the P_2-EMS contact, combined with the relatively fast recovery time, suggest that GPR-1 becomes enriched at the P_2-EMS contact by simple diffusion and binding to a site that increases its cortical stability, creating a diffusion trap (Gingell and Owens, 1992). The reciprocal changes at the P_2-EMS and P_2-ABp contacts (Fig. 6C)

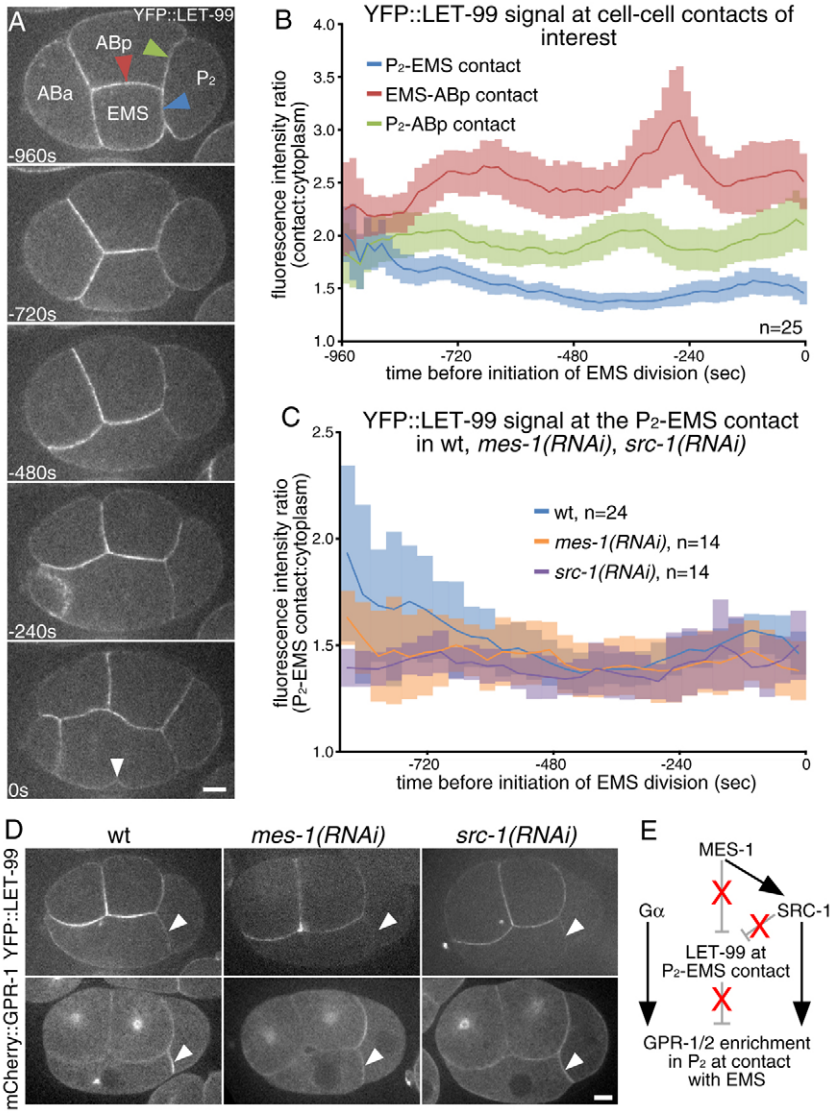

Fig. 5. MES-1/SRC-1 signaling localizes cortical GPR-1 independently of LET-99. (**A**) Live imaging of YFP::LET-99. Colored arrowheads mark cell contacts of interest. White arrowhead marks initiation of EMS division. (**B**) Quantification of YFP::LET-99 at cell contacts of interest. (**C**) YFP::LET-99 signal at the P_2-EMS contact becomes indistinguishable between wild-type, *mes-1(RNAi)* and *src-1(RNAi)* backgrounds. Error bars indicate 95% confidence intervals (**D**) mCherry::GPR-1 fails to become significantly enriched at P_2-EMS contact (arrowheads) in *mes-1(RNAi)* or *src-1(RNAi)* backgrounds (bottom), without YFP::LET-99 accumulating at this contact (top). Scale bars: 5 μm. (**E**) Proposed model for the role of MES-1/SRC-1 signaling in GPR-1 cortical enrichment.

suggest that the normal, asymmetric localization of this TPR-GoLoco protein is established by destabilization at one cell contact, diffusion and stabilization at another cell contact.

Microtubule-dependent removal of GPR-1/2 prevents excessive accumulation

Our results suggested that precise levels of GPR-1/2 may be important, as excess GPR-1/2 resulted in centrosome oscillations between the nucleus and the site of contact with EMS (Fig. 4) and some embryonic lethality that could be reduced by RNAi of endogenous protein (see Fig. S1 in the supplementary material). We noticed that after the peak level of GPR-1 at the P_2-EMS border was reached, the level decreased as the cells approached mitosis, both by transgene reporters and by immunostaining endogenous protein in wild-type embryos (Fig. 1E; see Fig. S1D, Fig. S3A,B in the supplementary material). This suggested that there might be a mechanism that removes GPR-1 upon spindle alignment, perhaps preventing GPR-1 from reaching an excessive level. The peak in GPR-1 asymmetry at cell-cell contacts occurred near the time when the P_2 centrosomes aligned toward the P_2-EMS contact (Fig. 7A,B). We found that as GPR-1 level dropped at the P_2-EMS contact, punctae of GPR-1 could be seen moving from the cell periphery toward the centrosomes, at a rate of 1.4±0.31 μm/sec (n=8) (Fig. 7C). Many punctae were seen coming off the P_2-EMS contact when centrosomes, and thus astral microtubules, were aligned toward the contact (Fig. 7D; see Movie 5 in the supplementary material). Endogenous GPR-1/2 could also be seen near astral microtubules by immunostaining (see Fig. S3C in the supplementary material), suggesting that these punctae are not an overexpression artifact.

These results suggested that cortical GPR-1/2 level at the P_2-EMS contact might be limited in normal development by microtubule-dependent removal of GPR-1/2 particles, in an apparent negative-feedback loop. To test this hypothesis, first, we treated embryos with nocodazole, which disrupted microtubules, and we quantified GPR-1 level at the P_2-EMS contact over time (Fig. 7E,F). We found that GPR-1 at this contact in nocodazole-treated embryos accumulated normally, but then the level failed to decrease at the time when spindle alignment would normally occur. Instead, the mCherry::GPR-1 level continued to increase at a linear rate similar to that before spindle alignment (Fig. 7F; see Movie 6 in the supplementary material). Second, we used a temperature-sensitive *spd-2* allele to compromise centrosome function (O'Connell et al., 2000; Kemp et al., 2004), and we found a similar

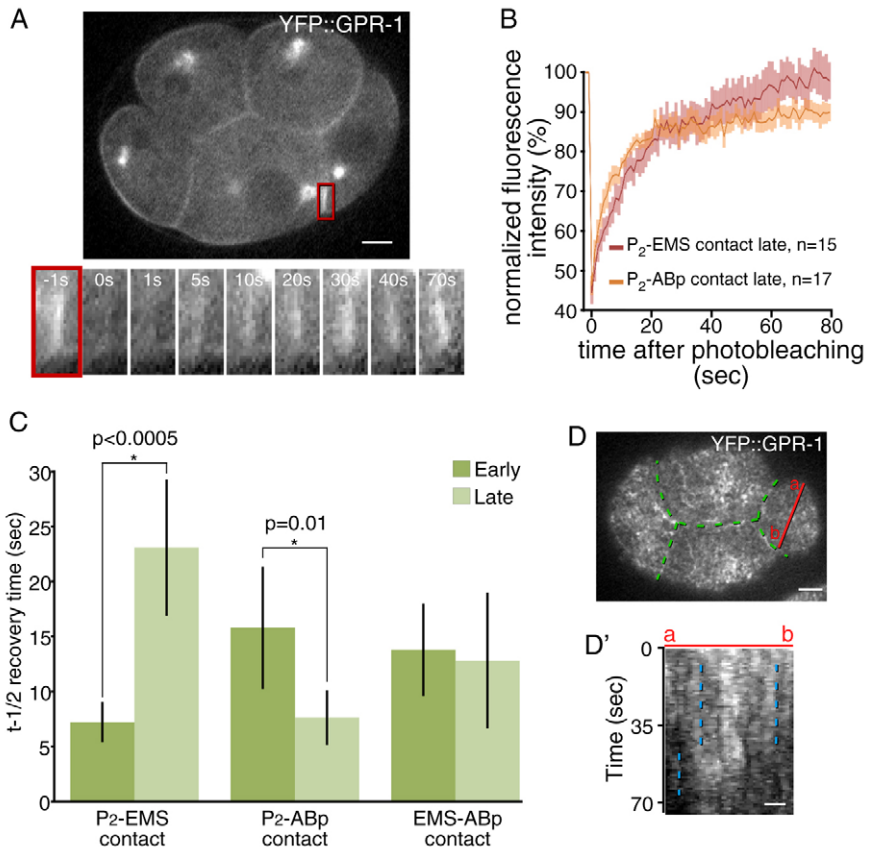

Fig. 6. Asymmetric localization of GPR-1 at the P_2-EMS contact is established by destabilization at one cell-contact site, diffusion and stabilization at another cell-contact site. (**A**) FRAP of the P_2-EMS contact at the late stage in the P_2 cell cycle. The region in the red box is expanded to show the photobleached area over time. (**B**) Average of multiple FRAP experiments (see also Fig. S6 in the supplementary material). Error bars indicate 95% confidence intervals. (**C**) Average half-life of recovery from one-phase exponentials fit to individual FRAP experiments. (**D**,**D′**) Punctae of YFP::GPR-1 near the upper surface of all cells at the four-cell stage. Broken green lines in D mark cell-cell contacts. Red line marks the region used to generate the kymograph in D′. Vertical broken blue lines mark cortical punctae of YFP::GPR-1, not moving toward the P_2-EMS contact. Scale bars: 5 μm in A,D; 2 μm in D′.

result (Fig. 7G,H). We conclude that removal of GPR-1/2 by microtubules, which are brought to the site of contact with EMS by spindle alignment, prevents further accumulation of GPR-1/2.

DISCUSSION

Intercellular communication leading to oriented cell divisions is a fundamental but poorly understood process in animal development and homeostasis. Here, we present the first high-resolution time-lapse imaging of a TPR-GoLoco protein that is involved in cell division orientation and that localizes in response to intercellular signaling. We show that GPR-1 is localized asymmetrically in a germline precursor cell. We demonstrate that the position to which GPR-1 localizes in this cell is determined by instructive MES-1/SRC-1 signaling, and we show biological roles for normal GPR-1/2 distribution in the P_2 cell. We tested whether MES-1/SRC-1 signaling affects GPR-1 localization through a known antagonist, LET-99, disproving this hypothesis. FRAP experiments showed that asymmetric localization is achieved by destabilization of GPR-1 at the site of contact between P_2 and ABp, diffusion and stabilization at the site of contact with EMS. Finally, we demonstrated that cortical accumulation of GPR-1 in P_2 at the site of contact with EMS is limited by microtubule-dependent removal. These results (Fig. 7I) indicate that the dynamic localization of TPR-GoLoco proteins can function as a key intermediate relaying positional information from intercellular signaling to the alignment of a mitotic spindle, and shed light on how TPR-GoLoco proteins are localized downstream of extracellular signaling.

Surprisingly, our work demonstrated GPR-1/2 is not asymmetrically enriched in EMS, although the cortical anchor of GPR-1/2, GPA-16, affects EMS spindle orientation (Tsou et al., 2003). This suggests that both GPR-1/2-asymmetry-dependent and GPR-1/2-asymmetry-independent mechanisms can affect spindle orientation. We speculate that even symmetrically localized GPR-1/2 can contribute to EMS spindle orientation if downstream binding partners in the TPR-GoLoco complex, such as dynein or LIN-5, are asymmetrically recruited or asymmetrically activated. In support of this, dynactin becomes enriched at the P_2-EMS contact downstream of both Wnt and Src signaling, and is required for EMS spindle alignment (Zhang et al., 2008). Similarly, Lis1/dynactin is important for spindle orientation in *Drosophila* neuroblasts (Siller and Doe, 2008).

It is also possible that symmetrical cortical TPR-GoLoco complexes can affect forces on microtubules throughout the cell cortex in a manner that permits additional asymmetric forces to be effective. MES-1 and Wnt signaling might result in asymmetric accumulation or activation of proteins in EMS that function in parallel to the TPR-GoLoco-complex. Based on studies in *C. elegans* and in other systems, the Wnt pathway proteins Dishevelled (DSH-2) and Frizzled (MOM-5) would be good candidates. DSH-2 is enriched at the P_2-EMS contact (Walston et al., 2004), is involved in spindle orientation in *C. elegans* early development, and has been shown to be involved in division orientation in other systems (Siller and Doe, 2008; Segalen et al., 2010). In addition, Frizzled shows Wnt-dependent asymmetric localization at a later stage in *C. elegans* development (Goldstein et al., 2006). Furthermore, Frizzled and Dishevelled form a complex with NuMA, the functional homolog of *C. elegans* LIN-5, and they can orient mitotic divisions during both *Drosophila* and zebrafish morphogenesis in a pathway parallel to the TPR-GoLoco force-generator pathway (Segalen et al., 2010).

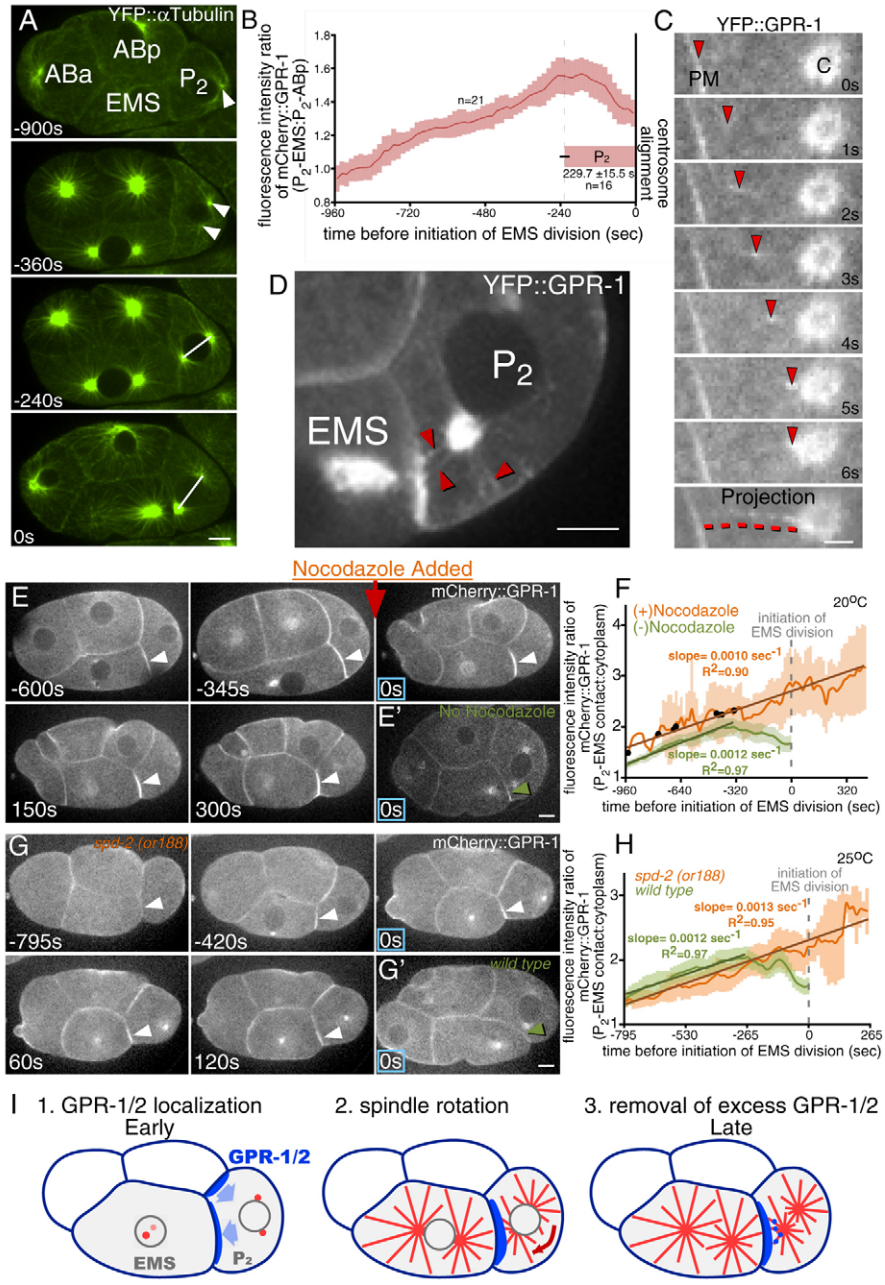

Fig. 7. Microtubule-dependent removal of cortical GPR-1 prevents excessive accumulation. (**A**) P_2 centrosomes (arrowheads) separated and aligned toward the P_2-EMS contact (white lines) by ~240 seconds before EMS division. (**B**) P_2 centrosomes first aligned near the time that GPR-1 asymmetry at cell-cell contacts peaked, then GPR-1 asymmetry decreased. (**C**) Puncta of YFP::GPR-1 (arrowheads) moving from the plasma membrane, PM, toward the centrosome, C. The projection shows all the panels above overlain. (**D**) Thirty-second projection of YFP::GPR-1. Arrowheads highlight tracks of multiple punctae moving toward a centrosome. (**E**) Nocodazole was added ~345 seconds before initiation of EMS division. Arrowheads indicate mCherry::GPR-1 at the P_2-EMS contact. (**E′**) An untreated embryo at initiation of EMS division shows weaker mCherry::GPR-1 accumulation at the P_2-EMS contact compared with a nocodazole-treated embryo at the same time point. (**F**) mCherry::GPR-1 continues to accumulates at the P_2-EMS contact at a comparable rate in nocodazole-treated (+) embryos as it does prior to centrosome alignment in untreated (–) embryos. Black dots represent times when individual nocodazole treatments began. Significantly more mCherry::GPR-1 accumulated at the P_2-EMS contact in nocodazole-treated embryos than in untreated embryos. At t=–15 seconds, contact:cytoplasm signal ratios were: untreated, 1.69±0.17 (n=21); nocodazole-treated, 2.77±0.36 (n=11); P<0.0001. (**G**) Live imaging of mCherry::GPR-1 in wild-type and *spd-2(or188)* embryos upshifted to 25°C just after birth of P_2 and EMS. Arrowheads indicate mCherry::GPR-1 at the P_2-EMS contact. (**G′**) A wild-type embryo expressing mCherry::GPR-1 shows weaker signal at the P_2-EMS contact compared with a similarly staged embryo from *spd-2(or188)*. (**H**) mCherry::GPR-1 continued to accumulate at the P_2-EMS contact in a *spd-2(or188)* background after the spindle would have normally oriented. At t=–15 seconds, contact:cytoplasm signal ratios of mCherry::GPR-1 were: wild-type *mCherry::gpr-1*, 1.60±0.13 (n=15); *mCherry::gpr-1; spd-2(or188)*, 2.21±0.28 (n=10); P=8.7×10^{-4}. (**I**) How GPR-1 asymmetric localization is destabilized at the P_2-EMS contact. (1) GPR-1 is destabilized at the P_2-ABp contact and stabilized at the P_2-EMS contact. Blue arrows represent net direction of GPR-1/2 diffusion. (2) Spindles in EMS and P_2 align. Red arrow indicates rotational movement in P_2. (3) Astral microtubules remove GPR-1 from the P_2-EMS contact. Scale bars: 2 μm in C; 5 μm in A,D,E,E′,G,G′. Error bars indicate 95% confidence intervals.

Previously in our lab, we used cell isolation experiments in which cells bearing MES-1 and Wnt signals from separate P_2 cells were placed at different locations on EMS cells (Goldstein et al., 2006). In these experiments, the EMS spindle aligned toward the Wnt-presenting cell and not the MES-1-presenting cell, suggesting that Wnt is an instructive cue and MES-1 is a permissive cue for EMS spindle alignment. However, in experiments presented here (Fig. 3A,D), the EMS spindle aligned only towards the MES-1^+/Wnt^+ cell and never toward the MES-1^-/WNT^+ cell. One possible explanation is that MES-1 and Wnt might together provide an instructional cue for spindle alignment that is more effective than the Wnt cue alone if both cues are presented from the same cell-cell contact.

In our recombination experiments, both centrosomes in EMS oriented toward both P_2 cells, as previously described (Goldstein, 1995), but only one centrosome P_2 oriented toward both EMS cells (Fig. 3A; see Movie 2 in the supplementary material). We speculate that the cell polarization mechanism of P_2, in which contact with EMS orients asymmetric PAR protein localization (Arata et al., 2010), might only allow cortical GPR-1/2 to accumulate in one side of the cell.

In *Drosophila* neuroblasts, the TPR-GoLoco protein Pins becomes asymmetrically localized at the cortex partly by delivery on astral microtubules (Siegrist and Doe, 2005). By contrast, during the four-cell stage of *C. elegans*, we show that GPR-1 localizes by diffusion, and microtubules act to limit, rather than to increase, cortical enrichment of GPR-1/2 (Figs 6, 7). These differences suggest that TPR-GoLoco proteins may become localized by multiple mechanisms. Based on our nocodazole and *spd-2* experiments (Fig. 7E-H; see Movie 6 in the supplementary material), we propose that, in *C. elegans*, excessive pulling forces on the P_2 mitotic spindle via excess GPR-1/2 might be avoided normally by microtubule-dependent removal of cortical GPR-1/2. The results suggest a negative-feedback loop in which GPR-1 levels are steadily accumulated at a site, resulting in pulling astral microtubules toward this site, whereupon GPR-1 levels are then moderated by these microtubules. Such a negative-feedback loop could serve to limit GPR-1/2 enrichment, preventing accumulation of GPR-1/2 to a level that might lead to defects such as the dissociation of a centrosome from the nucleus.

In conclusion, we demonstrate that the dynamic localization of GPR-1/2 can serve as a key intermediate, relaying positional information from intercellular signaling to the alignment of a mitotic spindle. Considered together with results from *Drosophila* (Gomes et al., 2009), our results demonstrate that TPR-GoLoco proteins can be localized by multiple intercellular signaling pathways. We speculate that orientation of mitotic spindles by intercellular signaling via TPR-GoLoco protein localization could be a fundamental and widespread mechanism by which cell division orientation is controlled in animal development.

Acknowledgements
We thank Lesilee Rose, Francois Schweisguth, Henrik Bringmann, Kerry Bloom, Vicki Bautch, Erin Osborne and past and present members of the Goldstein Lab for helpful discussions and comments on the manuscript. We thank Monica Gotta, Sander van den Heuvel and Lesilee Rose for sharing GPR-2 antibodies; Kevin O'Connell for sharing *spd-2(or188)*; and Henrik Bringmann for sharing mCherry::GPR-1, YFP::GPR-1 and YFP::LET-99 strains. Some nematode strains used in this work were provided by the Caenorhabditis Genetics Center.

Funding
This work was supported an NIH Cell & Molecular Biology Training Grant at UNC Chapel Hill and by NSF grant IOS-0917726 to B.G. Deposited in PMC for release after 12 months.

Competing interests statement
The authors declare no competing financial interests.

Supplementary material
Supplementary material for this article is available at
http://dev.biologists.org/lookup/suppl/doi:10.1242/dev.070979/-/DC1

References
Arata, Y., Lee, J. Y., Goldstein, B. and Sawa, H. (2010). Extracellular control of PAR protein localization during asymmetric cell division in the *C. elegans* embryo. *Development* **137**, 3337-3345.
Berkowitz, L. A. and Strome, S. (2000). MES-1, a protein required for unequal divisions of the germline in early *C. elegans* embryos, resembles receptor tyrosine kinases and is localized to the boundary between the germline and gut cells. *Development* **127**, 4419-4431.
Brenner, S. (1974). The genetics of *Caenorhabditis elegans*. *Genetics* **77**, 71-94.
Chen, W. S., Antic, D., Matis, M., Logan, C. Y., Povelones, M., Anderson, G. A., Nusse, R. and Axelrod, J. D. (2008). Asymmetric homotypic interactions of the atypical cadherin flamingo mediate intercellular polarity signaling. *Cell* **133**, 1093-1105.
Colombo, K., Grill, S. W., Kimple, R. J., Willard, F. S., Siderovski, D. P. and Gonczy, P. (2003). Translation of polarity cues into asymmetric spindle positioning in *Caenorhabditis elegans* embryos. *Science* **300**, 1957-1961.
Du, Q. and Macara, I. G. (2004). Mammalian Pins is a conformational switch that links NuMA to heterotrimeric G proteins. *Cell* **119**, 503-516.
Dudley, N. R., Labbe, J. C. and Goldstein, B. (2002). Using RNA interference to identify genes required for RNA interference. *Proc. Natl. Acad. Sci. USA* **99**, 4191-4196.
Edgar, L. G. (1995). Blastomere culture and analysis. *Methods Cell Biol.* **48**, 303-321.
El-Hashash, A. H., Turcatel, G., Al Alam, D., Buckley, S., Tokumitsu, H., Bellusci, S. and Warburton, D. (2011). Eya1 controls cell polarity, spindle orientation, cell fate and Notch signaling in distal embryonic lung epithelium. *Development* **138**, 1395-1407.
Galli, M. and van den Heuvel, S. (2008). Determination of the cleavage plane in early *C. elegans* embryos. *Annu. Rev. Genet.* **42**, 389-411.
Gingell, D. and Owens, N. (1992). How do cells sense and respond to adhesive contacts? Diffusion-trapping of laterally mobile membrane proteins at maturing adhesions may initiate signals leading to local cytoskeletal assembly response and lamella formation. *J. Cell Sci.* **101**, 255-266.
Goldstein, B. (1995). Cell contacts orient some cell division axes in the *Caenorhabditis elegans* embryo. *J. Cell Biol.* **129**, 1071-1080.
Goldstein, B., Takeshita, H., Mizumoto, K. and Sawa, H. (2006). Wnt signals can function as positional cues in establishing cell polarity. *Dev. Cell* **10**, 391-396.
Gomes, J. E., Corado, M. and Schweisguth, F. (2009). Van Gogh and Frizzled act redundantly in the *Drosophila* sensory organ precursor cell to orient its asymmetric division. *PLoS ONE* **4**, e4485.
Gotta, M., Dong, Y., Peterson, Y. K., Lanier, S. M. and Ahringer, J. (2003). Asymmetrically distributed *C. elegans* homologs of AGS3/PINS control spindle position in the early embryo. *Curr. Biol.* **13**, 1029-1037.
Grill, S. W., Gonczy, P., Stelzer, E. H. and Hyman, A. A. (2001). Polarity controls forces governing asymmetric spindle positioning in the *Caenorhabditis elegans* embryo. *Nature* **409**, 630-633.
Grill, S. W., Howard, J., Schaffer, E., Stelzer, E. H. and Hyman, A. A. (2003). The distribution of active force generators controls mitotic spindle position. *Science* **301**, 518-521.
Hao, Y., Du, Q., Chen, X., Zheng, Z., Balsbaugh, J. L., Maitra, S., Shabanowitz, J., Hunt, D. F. and Macara, I. G. (2010). Par3 controls epithelial spindle orientation by aPKC-mediated phosphorylation of apical Pins. *Curr. Biol.* **20**, 1809-1818.
Hill, D. P. and Strome, S. (1988). An analysis of the role of microfilaments in the establishment and maintenance of asymmetry in *Caenorhabditis elegans* zygotes. *Dev. Biol.* **125**, 75-84.
Hoffman, D. B., Pearson, C. G., Yen, T. J., Howell, B. J. and Salmon, E. D. (2001). Microtubule-dependent changes in assembly of microtubule motor proteins and mitotic spindle checkpoint proteins at PtK1 kinetochores. *Mol. Biol. Cell* **12**, 1995-2009.
Inaba, M., Yuan, H., Salzmann, V., Fuller, M. T. and Yamashita, Y. M. (2010). E-cadherin is required for centrosome and spindle orientation in *Drosophila* male germline stem cells. *PLoS ONE* **5**, e12473.
Kemp, C. A., Kopish, K. R., Zipperlen, P., Ahringer, J. and O'Connell, K. F. (2004). Centrosome maturation and duplication in *C. elegans* require the coiled-coil protein SPD-2. *Dev. Cell* **6**, 511-523.
Lechler, T. and Fuchs, E. (2005). Asymmetric cell divisions promote stratification and differentiation of mammalian skin. *Nature* **437**, 275-280.
McCarthy Campbell, E. K., Werts, A. D. and Goldstein, B. (2009). A cell cycle timer for asymmetric spindle positioning. *PLoS Biol.* **7**, e1000088.

Nguyen-Ngoc, T., Afshar, K. and Gonczy, P. (2007). Coupling of cortical dynein and G alpha proteins mediates spindle positioning in *Caenorhabditis elegans*. *Nat. Cell Biol.* **9**, 1294-1302.
O'Connell, K. F., Maxwell, K. N. and White, J. G. (2000). The spd-2 gene is required for polarization of the anteroposterior axis and formation of the sperm asters in the *Caenorhabditis elegans* zygote. *Dev. Biol.* **222**, 55-70.
Oliaro, J., Van Ham, V., Sacirbegovic, F., Pasam, A., Bomzon, Z., Pham, K., Ludford-Menting, M. J., Waterhouse, N. J., Bots, M., Hawkins, E. D. et al. (2010). Asymmetric cell division of T cells upon antigen presentation uses multiple conserved mechanisms. *J. Immunol.* **185**, 367-375.
Park, D. H. and Rose, L. S. (2008). Dynamic localization of LIN-5 and GPR-1/2 to cortical force generation domains during spindle positioning. *Dev. Biol.* **315**, 42-54.
Pease, J. C. and Tirnauer, J. S. (2011). Mitotic spindle misorientation in cancer-out of alignment and into the fire. *J. Cell Sci.* **124**, 1007-1016.
Pecreaux, J., Roper, J. C., Kruse, K., Julicher, F., Hyman, A. A., Grill, S. W. and Howard, J. (2006). Spindle oscillations during asymmetric cell division require a threshold number of active cortical force generators. *Curr. Biol.* **16**, 2111-2122.
Peyre, E., Jaouen, F., Saadaoui, M., Haren, L., Merdes, A., Durbec, P. and Morin, X. (2011). A lateral belt of cortical LGN and NuMA guides mitotic spindle movements and planar division in neuroepithelial cells. *J. Cell Biol.* **193**, 141-154.
Redemann, S., Schloissnig, S., Ernst, S., Pozniakowsky, A., Ayloo, S., Hyman, A. A. and Bringmann, H. (2010). Codon adaptation-based control of protein expression in *C. elegans*. *Nat. Methods* **8**, 250-252.
Rose, L. S. and Basham, S. E. (2006). *Caenorhabditis elegans* embryo: establishment of asymmetry. In *Encyclopedia of Life Sciences* doi: 10.1038/npg.els.0004224. John Wiley.
Sawyer, J. M., Glass, S., Li, T., Shemer, G., White, N. D., Starostina, N. G., Kipreos, E. T., Jones, C. D. and Goldstein, B. (2011). Overcoming redundancy: an RNAi enhancer screen for morphogenesis genes in *C. elegans*. *Genetics* **188**, 549-564.
Schlesinger, A., Shelton, C. A., Maloof, J. N., Meneghini, M. and Bowerman, B. (1999). Wnt pathway components orient a mitotic spindle in the early *Caenorhabditis elegans* embryo without requiring gene transcription in the responding cell. *Genes Dev.* **13**, 2028-2038.
Segalen, M. and Bellaiche, Y. (2009). Cell division orientation and planar cell polarity pathways. *Semin. Cell Dev. Biol.* **20**, 972-977.
Segalen, M., Johnston, C. A., Martin, C. A., Dumortier, J. G., Prehoda, K. E., David, N. B., Doe, C. Q. and Bellaiche, Y. (2010). The Fz-Dsh planar cell polarity pathway induces oriented cell division via Mud/NuMA in *Drosophila* and zebrafish. *Dev. Cell* **19**, 740-752.
Shelton, C. A. and Bowerman, B. (1996). Time-dependent responses to glp-1-mediated inductions in early *C. elegans* embryos. *Development* **122**, 2043-2050.
Siegrist, S. E. and Doe, C. Q. (2005). Microtubule-induced Pins/Galphai cortical polarity in *Drosophila* neuroblasts. *Cell* **123**, 1323-1335.
Siller, K. H. and Doe, C. Q. (2008). Lis1/dynactin regulates metaphase spindle orientation in *Drosophila* neuroblasts. *Dev. Biol.* **319**, 1-9.
Siller, K. H. and Doe, C. Q. (2009). Spindle orientation during asymmetric cell division. *Nat. Cell Biol.* **11**, 365-374.
Srinivasan, D. G., Fisk, R. M., Xu, H. and van den Heuvel, S. (2003). A complex of LIN-5 and GPR proteins regulates G protein signaling and spindle function in *C. elegans*. *Genes Dev.* **17**, 1225-1239.
Strome, S., Martin, P., Schierenberg, E. and Paulsen, J. (1995). Transformation of the germ line into muscle in mes-1 mutant embryos of *C. elegans*. *Development* **121**, 2961-2972.
Tenlen, J. R., Molk, J. N., London, N., Page, B. D. and Priess, J. R. (2008). MEX-5 asymmetry in one-cell *C. elegans* embryos requires PAR-4- and PAR-1-dependent phosphorylation. *Development* **135**, 3665-3675.
Thorpe, C. J., Schlesinger, A., Carter, J. C. and Bowerman, B. (1997). Wnt signaling polarizes an early *C. elegans* blastomere to distinguish endoderm from mesoderm. *Cell* **90**, 695-705.
Tsou, M. F., Hayashi, A. and Rose, L. S. (2003). LET-99 opposes Galpha/GPR signaling to generate asymmetry for spindle positioning in response to PAR and MES-1/SRC-1 signaling. *Development* **130**, 5717-5730.
Walston, T., Tuskey, C., Edgar, L., Hawkins, N., Ellis, G., Bowerman, B., Wood, W. and Hardin, J. (2004). Multiple Wnt signaling pathways converge to orient the mitotic spindle in early *C. elegans* embryos. *Dev. Cell* **7**, 831-841.
Williams, S. E., Beronja, S., Pasolli, H. A. and Fuchs, E. (2011). Asymmetric cell divisions promote Notch-dependent epidermal differentiation. *Nature* **470**, 353-358.
Zhang, H., Skop, A. R. and White, J. G. (2008). Src and Wnt signaling regulate dynactin accumulation to the P2-EMS cell border in *C. elegans* embryos. *J. Cell Sci.* **121**, 155-161.
Zheng, Z., Zhu, H., Wan, Q., Liu, J., Xiao, Z., Siderovski, D. P. and Du, Q. (2010). LGN regulates mitotic spindle orientation during epithelial morphogenesis. *J. Cell Biol.* **189**, 275-288.

Table S1. Strains used

Strain	Genotype	Name given in article	Source
N2	Wild type	Wild type	*Caenorhabditis* Genetics Center
TH242	*unc-119(ed3)* III; ddIs32[*yfp::gpr-1*(synthetic, CAI 1.0, artificial introns); *unc-119*(+)]	YFP::GPR-1	A gift from H. Bringmann, (Redemann et al., 2010)
TH384*	*unc-119(ed3)* III; ddIs79[*mCherry::gpr-1*(synthetic, CAI 1.0, artificial introns) *unc-119*(+)]	mCherry::GPR-1	A gift from H. Bringmann
SS149	*mes-1(bn7)*		Capowski et al., 1991
LP42	TH384; *mes-1(bn7)*	*mes-1(bn7)*; mCherry::GPR-1	This paper
LP43	TH384; *mom-2(or309)/nT1*		This paper
LP44	TH384; *gpa-16(it143)*		This paper
LP45	TH384; TH65	mCherry::GPR-1; YFP::alpha tubulin	This paper
LP46	TH384; *spd-2(or188)*	mCherry::GPR-1; *spd-2(or188)*	This paper
TH73	*yfp::let-99*	YFP::LET-99	Bringmann et al., 2007
TH65	*yfp::α-tubulin*	YFP::α-tubulin	Kozlowski et al., 2007
	gfp::gpr-2	GFP::GPR-2	Colombo et al., 2003

*This strain was received as an extrachromosomal array and was integrated in our laboratory.

Additional references

Bringmann, H., Cowan, C. R., Kong, J. and Hyman, A. A. (2007). LET-99, GOA-1/GPA-16, and GPR-1/2 are required for aster-positioned cytokinesis. *Curr. Biol.* **17**, 185-191.

Capowski, E. E., Martin, P., Garvin, C. and Strome, S. (1991). Identification of grandchildless loci whose products are required for normal germline development in the nematode Caenorhabditis elegans. *Genetics* **129**, 1061-1072.

Kozlowski, C., Srayko, M. and Nedelec, F. (2007). Cortical microtubule contacts position the spindle in C. elegans embryos. *Cell* **129**, 499-510.